INFLUENCE OF DESIGN CONDITIONS ON THE DISTRIBUTION OF OPTIMAL WINDOW TO WALL RATIO FOR A TYPICAL OFFICE BUILDING IN JAPAN

Liwei Wen[1], Kyosuke Hiyama[2]
[1, 2] Faculty of Engineering, Yamaguchi University, Ube-shi, Japan

ABSTRACT

This paper simulates a typical Japanese open office building to investigate the influence of design conditions on the distribution of optimal window-to-wall ratio (WWR). Results are expected to be adopted to create a recommended WWR range map for default value assignment in early performance simulations. The impact of lighting power density, climate conditions, window orientation, internal gain, and building scale are investigated. Results are discussed under the normal lighting power density of 10 W/m^2 and an assumed value of 5 W/m^2. A larger WWR is liable to be advantageous for CO_2 emission reduction under the normal lighting power density in the main island of Japan. However, the distribution of optimal WWR is found to be sensitive to all the investigated design conditions when the lighting power density is reduced. A comparison study demonstrates that internal gain and building scale can be regarded as minimal influential conditions. Climate conditions and window orientation should be considered in the future map creation.

INTRODUCTION

It is widely recognized that design decisions, such as building shape and envelope properties, made in the early design stage significantly influence building performance (Hong et al., 2000, Morbitzer et al., 2001, Granadeiro et al., 2013). To realize net zero energy building, building performance simulation should be carried out as early as possible in the design process to verify design decisions (Attia et al., 2011). The American Institute of Architects (AIA) published a design guideline to encourage architects to integrate energy/performance modeling into the design process (AIA, 2012). This guideline named the early energy/performance prediction as Design Performance Modeling (DPM).

The development of building information modeling (BIM) technology accelerates and simplifies the input of geometry data in simulation. However, building properties data (non-geometry data) are still difficult to deal with in the early design stage when the detailed building information is still unknown (Cerezo et al., 2014). Modeling scenarios are performed to illustrate the crucial influence of input quality and availability on predicted results and decision-making (Bazjanac et al., 2011). Therefore, an effective approach for determining inputs is necessary to popularize the use of DPM. For example, window area, expressed as WWR, simultaneously affects daylight use and solar thermal load and is considered to be an influential design variable in office buildings (Pino et al., 2012). In addition, it is also a necessary input demanded by DPM (Grinberg, 2013); thus, this study focuses on the approach for assigning default value of WWR.

BIM data accumulated from past projects can provide suggestions for simulating a new project (Hiyama et al., 2014). The definition and importance of default value are supplemented in a following research (Hiyama, 2014). Of note, it is difficult to select an appropriate reference data among a large amount of data, unless the architects are sufficiently knowledgeable and experienced. The awareness of design parameters for determining the similarity between a new project and reference projects is necessary for architects when reusing BIM data. In this context, it is useful to show architects a map marked with recommended WWR ranges so that they can find an optimal solution according to the contents of their new project. It is expected that this map will be created from the results of optimization calculation under the design conditions having a major effect on the distribution of optimal WWR.

This study examines an integrated thermal and daylight analysis of a typical open office building in Japan under different design conditions. The main purpose of this study is to investigate the influence of design conditions on the distribution of optimal WWR. The results from this study can be furtherly adopted to determine the type of building to use for assigning the default value of a new project.

METHODOLOGY

The methodology is based on the analysis of different case studies. Each case study is performed under a particular design condition: an open office is simulated using lighting power densities of 10 W/m^2 and 5 W/m^2 with variable climate conditions, window orientation, internal gain, and building scale.

Simulation scheme

A typical Japanese five-story open office building is adopted for this study’s simulation (Takizawa 1984). Figures 1 and 2 show the 3D model and the floor plan of the small-scale building model, respectively. It is assumed that only one glazed façade is installed in each zone. Thus, external windows of the building model would face north and south, or east and west. Table 1 lists the thermal properties of construction element and HVAC system settings. DesignBuilder integrating EnergyPlus calculation engine is used for simulation (DesignBuilder versions 4, 2014). The desirable illuminance on the work plan is set at 400 lx. A continuous dimming control is selected to correspond with the utilization of daylight. Figure 2 also shows the location of two daylight sensors in each zone. The 3rd floor is chosen as the simulation object. The design variable is WWR varying from 10 to 70 % with an interval of 10 %. The objective function is the annual CO_2 emissions. In this study, the annual CO_2 emissions are from electricity consumption used for cooling/heating and lighting.

Variable design conditions

Table 2 describes the five investigated design conditions. In total, 72 case studies are performed with the five variable design conditions. Two lighting power densities of 10 W/m^2 and 5 W/m^2 are used in simulation. The former density represents the current level in typical office buildings and the latter one is an assumed level achieved by the development of lighting efficiency and control system. The Expanded AMeDAS Weather Data of Sapporo, Tokyo and Naha are adopted in simulation to consider the impact of climate conditions. The mean external temperatures of three cities are 8.8 °C, 16.6 °C and 23.3 °C respectively. It is mentioned that windows of building should face north and south or east and west. Moreover, the simulated results are individually collected from Zones 1 and 2. Thus, the influence of each window orientation can be examined. Internal gain is assumed to be a combination of heat gain from occupancy and equipment. Internal gain varies at three levels: low, medium, and high. Medium internal gain is regarded as the current normal level in typical Japanese office buildings. On both the small and large-scale, simulation buildings are conceived to discuss the effect of space depth.

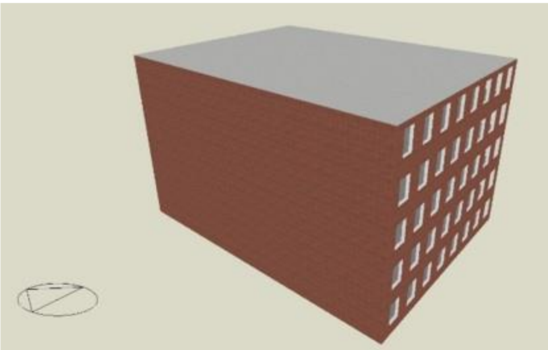

Figure 1 3D model of small-scale building

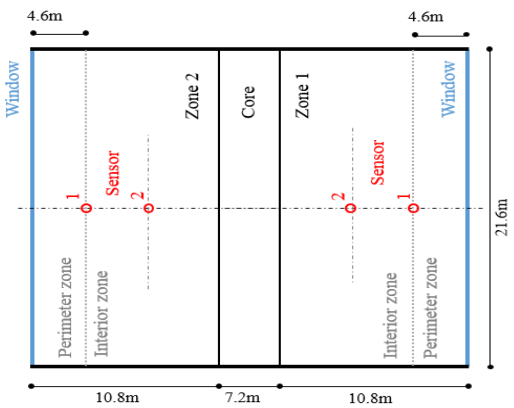

Figure 2 Floor plan detailing daylight sensor locations of a small-scale building

Table 1. Simulation conditions

U-value of construction elements	External wall: 0.55 W/m^{2}K
	Roof: 0.46 W/m^{2}K
	Ground floor: 0.87 W/m^{2}K
	Internal floor: 1.13 W/m^{2}K
	Internal partition: 2.43 W/m^{2}K
Window properties	Clear Low-E Double-pane, U-value: 1.8 W/m^{2}K, SHGC: 0.56,VT: 0.75
Window shading	Blind with high reflectivity slats (inside), Solar control, Set-point: 120 W/m^2
HVAC	Electricity form grid (carbon emission factor: 0.685 kgCO_2/kWh) Heating System CoP: 2*, Heating set-point temperature: 20 °C. Cooling System CoP: 3*, Cooling set-point temperature: 28 °C, Schedule: off-8:00-on-18:00-off, Mechanical ventilation: 7 l/s-person

** This value referred to the annual evaluation value of multi-split type (VRV system) air conditioning (Hiraoka et al., 2011)*

RESULTS AND DISCUSSION

Results under lighting power density of 10 W/m^2

Figures 3 (a), (b), and (c) show the relationship between CO_2 emissions and WWR in Sapporo, Tokyo, and Naha when the design conditions of small-scale building with medium internal gain are selected. The optimal WWR values of cases in Figure 3 are summarized in Table 3. Figure 3 (a) demonstrates that CO_2 emissions of the Sapporo building continually decrease with the increasing WWR, regardless of window orientation. In comparison with other three orientations, the decreasing tendency of CO_2 emissions with a south- facing orientation is more obvious. Similar decreasing tendencies of CO_2 emissions with the rise in window area can also be observed in the north- and west-facing orientations in Tokyo, as shown in Figure 3 (b). While CO_2 emissions in south- and east-facing orientations initially decrease, a slight rising tendency is subsequently exhibited once the WWR exceeds a certain value. The values of optimal WWR are decided as 60 % and 50 % in south and east orientation in Tokyo (Table 3). When WWR

Table 2 Description of variable design conditions

Lighting power density	10 W/m^2 (2.5 W/m^2-100 lx), 5 W/m^2 (1.25 W/m^2-100 lx) Schedule: 0%-9:00-80%-12:00-56%-13:00-80%-18:00-40%-20:00-0%,
Climate conditions	Sapporo, Tokyo, Naha
Window orientation	North and South, East and West
Internal gain	Low internal gain: occupancy density of 0.1 W/m^2, equipment density of 10 W/m^2 Medium internal gain: occupancy density of 0.2 W/m^2, equipment density of 20 W/m^2 High internal gain: occupancy density of 0.4 W/m^2, equipment density of 40 W/m^2 Occupancy schedule: 0%-9:00-70%-12:00-35%-13:00-70%-17:00-35%-18:00-17%-19:00-0%, Equipment schedule: 0%-9:00-50%-12:00-25%-13:00-50%-17:00-25%-18:00-0%
Building scale	Small-scale: space depth of 10.8 m, floor area of 622 m^2 (233 m^2 in a signal zone) Large-scale: space depth of 18 m, floor area of 1555 m^2 (648 m^2 in a signal zone) Space depth: distance between the external windows and the internal partition in each zone

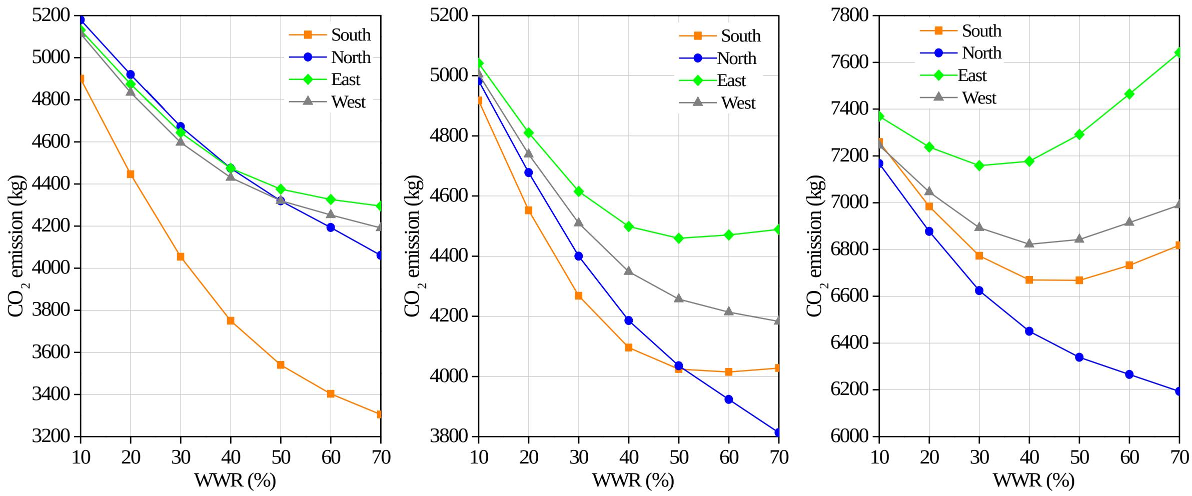

(a) Sapporo *(b) Tokyo* *(c) Naha*

Figure 3 Impact of climate conditions and window orientation in the case of medium internal gain and small-scale building

Table 3 Optimal WWR values in the cases of medium internal gain and small-scale building

	Sapporo	Tokyo	Naha
South	70 %	60 %	50%
North	70 %	70 %	70 %
East	70 %	50 %	30 %
West	70%	70 %	40 %

is in excess of optimal values for these two orientations, however, CO_2 emissions increase in increments less than 1 %. Thus, it is robust enough to consider that a larger WWR is recommended for CO_2 emission reduction, even for southern and eastern exposures in Tokyo.

Figure 3 (c) presents the variation in CO_2 emissions with the window area in Naha where solar radiation is relatively high. Because of a high cooling demand in Naha, CO_2 emissions are remarkably higher than that of the two other cities. Furthermore, the varying tendencies of CO_2 emissions with window areas in Naha also differ from Sapporo and Tokyo. Initially, CO_2 emissions decrease with WWR, varying from 10 % to the optimal WWR, and even reversely resulting in an increase as WWR increased, with the exception of a northern orientation. The values of an optimal WWR in the three orientations differ from each other but mainly range between 20 and 60 % (Table 3). The decreasing CO_2 emissions with WWR can be seen in the northern orientation of Naha. It is summarized that the distribution of optimal WWR is sensitive to the window orientation in Naha.

The tendency for CO_2 emissions to decrease parallel to WWR in Figures 3 (a) and (b) is explained using the example of the east-facing orientation in Sapporo. Figure 4 (a) shows the increment in CO_2 emissions from cooling, heating, and lighting at every 10 % increment in WWR. The CO_2 emissions from cooling increase with a rise in WWR; the reason for this is that the cooling demand is increased due to the high solar gain and heat transmittance. Conversely, CO_2 emissions from lighting decrease with a rise in the window area in accompany with daylight usage. Despite a slight variation, it can also be observed in the CO_2 emissions from heating. It is clear that the optimal WWR is mainly dependent on the relation between the rise in the CO_2 emissions from cooling and the reduction in CO_2 emissions from lighting induced by the increased window area. In the cases of Sapporo and Tokyo, the decrease in CO_2 emissions from lighting is always larger than or equal to the increase in CO_2 emissions from cooling.

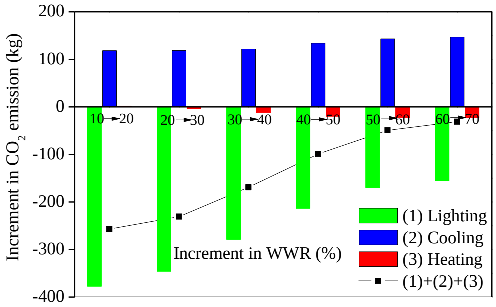

(a) Eastern exposure in Sapporo

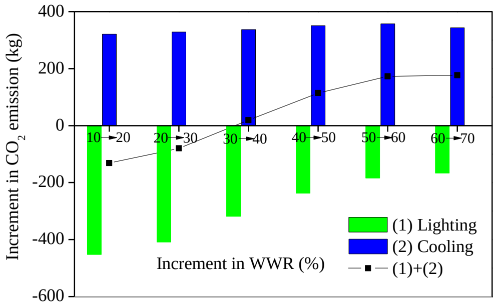

(b) Eastern exposure in Naha

Figure 4 Increment in CO_2 emissions from cooling, heating, and lighting at every 10 % increment in WWR

(Medium internal gain and small- scale building)

Geographic location is an influential factor governing climate conditions. The latitudes varying from Sapporo to Tokyo cover almost all the possible ranges in the main island of Japan. However, Naha with relatively low latitude is far from the main island. It is inferred that the influence of climate conditions on the distribution of optimal WWR is negligible in the majority of main island Japan. Moreover, a larger window area is advantageous irrespective of window orientation.

Figure 4 (b) analyzes CO_2 emissions originating from the cooling and lighting of an east façade to explain the distribution of optimal WWR for Naha. The increasing tendency of CO_2 emissions from cooling and decreasing tendency of CO_2 emissions from lighting in Naha are similar to those in Figure 4 (a). The decrement of CO_2 emissions from lighting is larger than the increment of CO_2 emissions from cooling at low WWR levels. An inflection point in corresponding to the optimal WWR appears as the WWR sequentially increases. At this point, the variation in CO_2 emissions from lighting is equivalent to that of cooling. The increment of CO_2 emissions from cooling becomes predominant as the WWR continues to increase. Therefore, an excessively large window is disadvantageous for CO_2 emission reduction in the exception of the northern exposure.

Figure 5 describes the plot of CO_2 emissions against the WWR at low, medium, and high internal gains for an east façade in Naha. The total CO_2 emissions markedly increase as the internal gain is improved. The level of internal gain, however, influences the distribution of optimal WWR less. An optimal WWR exists within the range of 20 and 60 % for the three cases. The optimal WWR values of cases in three cities at three levels of internal gain are summarized in Table 4. The change in the optimal WWR value at different levels of internal gain is no more than 10 % in the cases of Tokyo and Naha, and nearly zero for Sapporo. Simulated results indicate that the distribution of optimal WWR is less sensitive to internal gain.

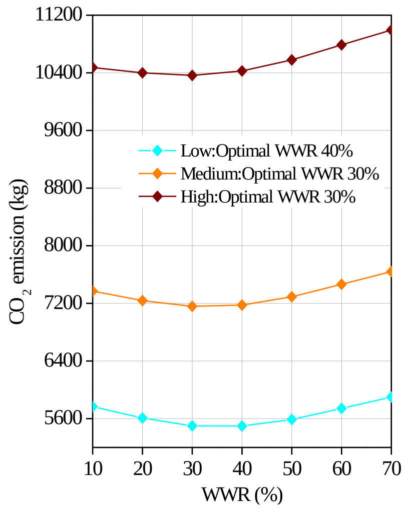

Figure 5 Impact of internal gain in the case of eastern exposures, Naha, and small-scale building

Table 4 Influence of internal gain on optimal WWR values in the case of small-scale building

		South	North	East	West
Sapporo	Low	70 %	70%	70%	70%
	Medium	70%	70%	70%	70%
	High	70%	70%	70%	70%
Tokyo	Low	60%	70%	60%	70%
	Medium	60%	70%	50%	70%
	High	50%	70%	50%	70%
Naha	Low	50%	70%	40%	40%
	Medium	50%	70%	30%	40%
	High	40%	70%	30%	40%

Decreasing tendencies of CO_2 emissions accompanied with the WWR are similar for all cases in three cities in simulated conditions of large-scale building (space depth of 18 m). A comparative study can be made between Figures 3 (c) and 6 to examine the effect of building scale on the distribution of optimal WWR. The inflection point on the simulation curves disappears in the south, west and east originations. The largest possible window area is recommended for all the cases, regardless of climate conditions and window orientation. Table 5 lists the optimal WWR values of cases in three cities at three internal gain levels using large-scale building. It is clear that internal gain even has no influence on the optimal WWR value with the exception to eastern exposure in Naha at high internal gain level. For this case, optimal WWR value is 50 %. However, it is found that the rise in total CO_2 emissions is around 1 %, even when the WWR is increased to 70 %. It is revealed that the impact of climate conditions, window orientation, and internal gain on the distribution of optimal WWR becomes less important for the strategy of increasing building scale. Decreasing CO_2 emissions from lighting always dominate even in the circumstance that solar radiation and internal gain are high. The reason is speculated that a zone with a deep space depth has great potential for daylight to reach the inner working plan through windows. Thus, the largest possible WWR is the best solution for a large-scale building with a large space depth.

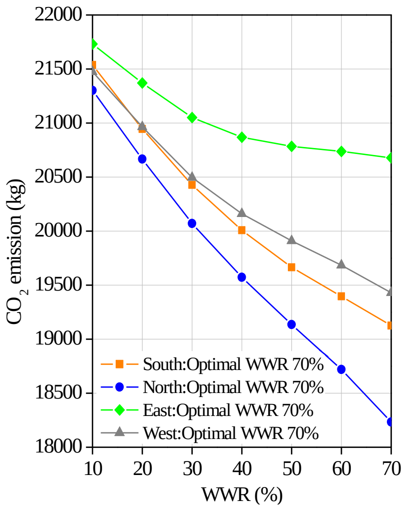

Figure 6 Simulation results in the case of Naha, medium internal gain, and large-scale building

Table 5 Influence of internal gain on optimal WWR values in the case of large-scale building

		South	North	East	West
Sapporo	Low	70%	70%	70%	70%
	Medium	70%	70%	70%	70%
	High	70%	70%	70%	70%
Tokyo	Low	70%	70%	70%	70%
	Medium	70%	70%	70%	70%
	High	70%	70%	70%	70%
Naha	Low	70%	70%	70%	70%
	Medium	70%	70%	70%	70%
	High	70%	70%	50%	70%

Results under lighting power density of 5 W/m^2

Developments in high efficiency lighting equipment, control system have extensively reduced lighting power density. In simulation, lighting power density is assumed at 5 W/m^2 in consideration of improved future lighting conditions. To simplify this explanation, the representative simulation results are displayed to understand the effect of design conditions on the distribution of optimal WWR.

Figure 7 shows the influence of climate conditions on the distribution of optimal WWR using the simulation model for a southern façade of a small-scale building at medium internal gain. It is distinctive that three different tendencies can be observed for the distribution of optimal WWR. (1) The larger the WWR is, the lower Sapporo CO_2 emissions become. (2) An optimal WWR can be identified within the range of 20 to 60 % in Tokyo. (3) It is interesting to note that CO_2 emissions in Naha constantly increase with increasing WWR. The smallest window area is the best choice in term of CO_2 emission reduction. The simulation results clearly indicate that the distribution of optimal WWR is sensitive to climate conditions.

Figure 8 presents the impact of window orientation on the distribution of optimal WWR when the conditions of Tokyo, medium internal gain, and small-scale are selected. With a northern façade, CO_2 emissions continually reduce as window area increases; the decreasing tendency gradually diminishes. However, in the remaining three orientations the remarkable inflection points can be seen in the range between 20 and 60 %. Thus, the consideration of orientation in window area design cannot be neglected.

Figure 9 reveals the effect of internal gain on the distributed of optimal WWR in the simulated case of an eastern façade on a small-scale building that is adopted in Tokyo. It is clear that total CO_2 emissions markedly increase as the internal gain is increased. The decreasing tendency of optimal WWR with the rise in internal gain can also be observed. However, at low and medium internal gains, an optimal WWR exists in the range of 20–60 %. The CO_2 emissions monotonically increase with the rise in WWR without the appearance of an inflection point once the internal gain improved to a high level. It is obvious that not only the optimal WWR value, but also the distribution of optimal WWR, is alerted with the variable level of internal gain.

Figure 10 exhibits the influence of building scale on the distribution of optimal WWR in the context of a northern façade and medium internal gain in Naha. For small-scale building, CO_2 emissions continually tend to increase with the rise in WWR. This is especially true when the WWR is in excess of 30 % and the increasing tendency accelerates. The relationship between CO_2 emissions and WWR becomes opposite to that of large-scale building. As the building scale increases, the largest WWR becomes optimal value. Thus, it is noted that the distribution of optimal WWR is dependent on the building scale.

The above simulation results under 5 W/m^2 well explain that the distribution of optimal WWR is sensitivity to all the investigated design conditions. Thus, it is useful to show architects a recommended

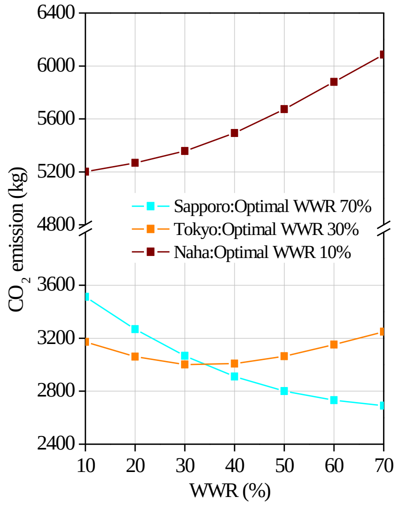

Figure 7 Impact of climate conditions in the case of southern exposures, medium internal gain, and small-scale building

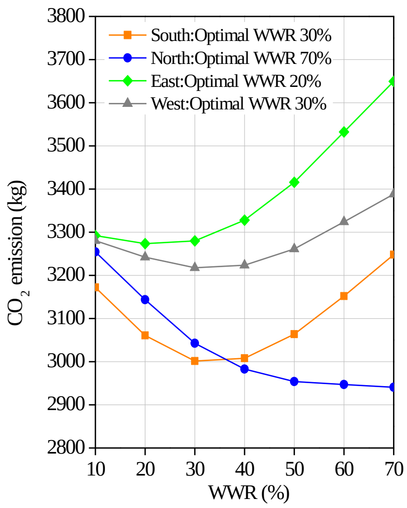

Figure 8 Impact of window orientation in the case of Tokyo, medium internal gain, and small-scale building

WWR range map for default value assigning in DPM. In order to create this map under the most influential design conditions, a further analysis on the impact originated from variable internal gain and building scale is performed.

Design conditions with minimal effect are considered to minimize the variation in objective function when the design conditions are changed. Thus, the analysis is based on the comparison of variation in CO_2 emissions when default value varies due to the change of internal gain or building scale conditions. The analysis process is illustrated using the results shown in Figures 9 and 10. The variation in CO_2 emissions E is calculated in Eq. (1).

$$E = \frac{Q_{ref} - Q_{min}}{Q_{min}} \times 100\% \quad (1)$$

Where, Q_{ref} is CO_2 emissions determined at a reference default value (kg), Q_{min} is CO_2 emissions determined

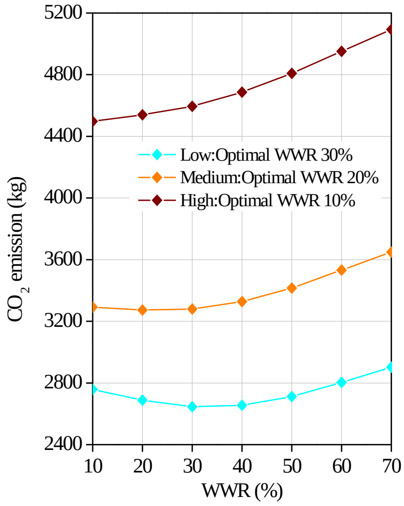

Figure 9 Impact of internal gain in the case of eastern exposures, Tokyo, and small-scale building

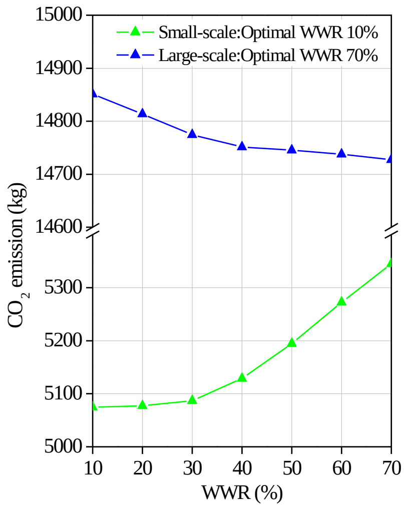

Figure 10 Impact of building scale in the case of northern exposures, Naha, and medium internal gain

at default value (kg), Q_{min} is CO_2 emissions determined at the optimal default value (kg).

In the case of internal gain (e.g. Figure 9), the optimal WWR obtained from the simulation results at medium internal gain is defined as the reference default value (20 %). The reason is that the medium internal gain approximately conforms to conditions of current typical office in Japan. The optimal default value is just the optimal WWR simulated under their respective simulation condition. Specifically, the optimal default values of low and high internal gains are 30 % and 20 %. Using $Q_{ref} - Q_{min}$, the increment in CO_2 emissions due to the default value varying from optimal default value to the reference default value can be calculated. The increment in CO_2 emissions is divided by the minimum CO_2 emissions to make E a dimensionless value. The calculation results show that the maximum variation in CO_2 emissions E are decided as 1.6% and 1% when the optimal default values at low and high levels of internal gain are replaced by the reference default value obtained from medium internal gain.

In terms of building scale (e.g. Figure 10), the reference default value is the optimal WWR decided at the small-scale building (10 %). Obviously, for large-scale building the optimal default value is 70 %. The maximum variation in CO_2 emissions E is less than 2 % when the reference default value obtained from small-scale building is assigned to the large-scale building.

The simulation results mentioned above confirm that the internal gain and building scale affect the distribution of optimal WWR in some cases. However, there is no obvious variation in CO_2 emissions when the optimal WWR values obtained from medium internal gain and small-scale building are assigned to the cases at low and high levels of internal gain and the case of large-scale building. It is believed that such a negligible variation in objective function would not cause a severe problem in building design. Internal gain and building scale can be regarded as minimal influential conditions in feature map creation. The optimization results under the conditions of medium internal gain and small-scale can be adopted by the buildings with variable conditions of integral gain and building scale.

CONCLUSION

This study simulates a typical Japanese open office building to investigate the influence of design conditions on the distribution of optimal WWR. The impact of lighting power density, climate conditions, window orientation, internal gain, and building scale are examined. Simulation results show that lighting power density plays a significant role in deciding the distribution of optimal WWR. Thus, the simulation results are discussed under the normal lighting power density (10 W/m^2) and an assumed lighting power density (5 W/m^2).

Design conditions do not significantly influence the distribution of optimal WWRs under normal lighting power density (10 W/m^2) condition. Some meaningful guidance, however, is obtained through simple case studies carried out in this research. It is noted that all the conclusions are obtained with the adoption of well insulated glazing (LoE glass) and solar shading. Noteworthy is that this research revealed that climate conditions do have an impact on the distribution of optimal WWR. A larger WWR is the best solution for the majority of areas on the main island of Japan regardless of window orientation.

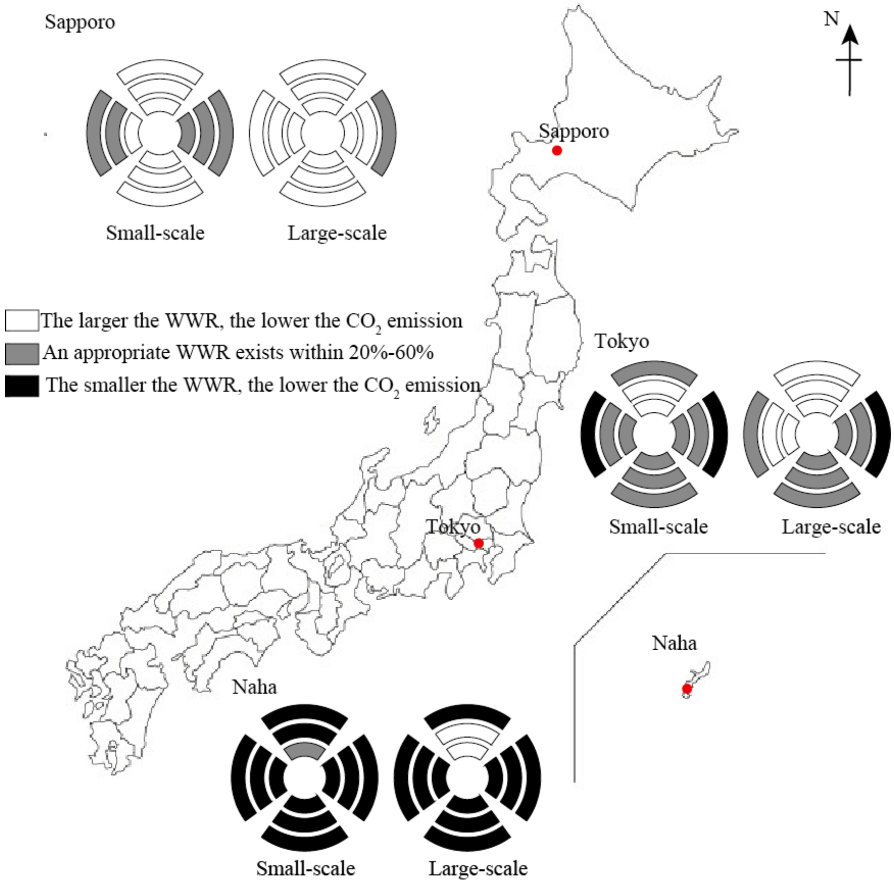

Figure 11 Impact of design conditions on the distribution of optimal WWRs under lighting power density of 5 W/m^2

(Doughnut from interior to exterior express low, medium, and high internal gain. The upper, lower, left, and right portions in one doughnut express the north, south, west, and east window orientation)

However, regarding the climate conditions with high solar radiation, such as Okinawa area, an appropriate WWR exists between the range of 20 and 60 %, with the exception of northern orientation. Furthermore, the impact of climate conditions gradually disappear as the space depth is enlarged for a large-scale building. Simulation results also express that internal gain has a negligible impact on the distribution of optimal WWR for all cases under normal lighting power density.

In the condition of the assumed lighting power density (5 W/m^2) induced by the development of lighting efficiency and control system, the distribution of optimal WWR can be generally divided into three types. (1) The larger the WWR is, the lower CO_2 emissions become. (2) An appropriate WWR exists within the range of 20 and 60 %. (3) The smaller the WWR is, the lower are the CO_2 emissions. Figure 11 summarizes the influence of design conditions on the distribution of optimal WWRs. It is clear that all the investigated conditions affect the distribution of optimal WWRs. The determination on the distribution of optimal WWRs becomes complicated. It is necessary, therefore, to provide a recommended WWR rang map for default value assignment regarding the future lighting conditions. However, obvious variations in CO_2 emissions is not seen when the optimal WWR values obtained at medium internal gain and small-scale are assigned to other cases at different levels of internal gain and large-scale building. It is accepted, therefore, that internal gain and building scale can be regarded as minimal influential conditions. Climate conditions, and window orientation should be carefully considered in the creation of the recommended WWR range map in our future research.

ACKNOWLEDGEMENT

This work was supported by Grant number 25709051.

REFERENCES

AIA. 2012. An architect's guide to integrating energy modeling in the design process. The American Institute of Architects

Attia, S., De Herde, A. 2011. Early design simulation tools for net zero energy buildings: a comparison of ten tools. 12th Conference of International Building Performance Simulation association, Sydeny, November 14-16.

Bazjanac, V., Maile, T., Rose, C., Donnell, J. T. O., Mrazovie, N., Morrissey, E., Welle, B. R. 2011. AN ASSESSMENT OF THE USE OF BUILING ENERGY PERFORMANCE SIMULATION IN EARLY DESIGN. 12th Conference of International Building Performance Simulation Association, Sydency, November 14-16.

Cerezo, C., Dogan, T., Reinhart, C. 2014. TOWARDS STANDARIZED BUILDING PROPERTIES TEMPLATE FILES FOR EARLY DESIGN ENERGY MODEL GENERATION. 2014 ASHRAE/IBPSA-USA: Building Simulation Conference Atlanta, GA, September 10-12.

DesignBuilder Software, " Design Builder," http://www.designbuilder.co.uk/.

Granadeiro, V., Correia, J. R., Leal, V. M. S., Duarte, J. P. 2013. Envelope-related energy demand: A design indicator of energy performance for residential buildings in early design stages. Energy and Buildings, 61, 215-223.

Grinberg, M., Rendek, R. 2013. ARCHITECTURE & ENERGY IN PRACTICE : IMPLEMENTING AN INFORMATION SHARING WORKFLOW. 13th Conference of International Building Performance Simulation Association, Chambery, France, August 26-28.

Hiraoka, M., Hiromoto, S., Komoda, H., Tabuchi, S., Tanabe, S., Kai, T., Hashimoto, S., Nishino, A. 2011 Performance Evaluation of Multi-split Type Air-conditioning System and Advancing Knowledge of HVAC Design. The Society of Heating, Air-Conditioning Sanitary Engineers of Japan, 169, 13-20.

Hiyama, K. 2014. Assigning Robust Default Values in Building Performance Simulation Software for Improved Decision-Making in the Initial Stages of Building Design. The Scientific World Joiurnal, 1-11.

Hiyama, K., Kato, S., Kubota, M., Zhang, J. 2014. A new method for reusing building information models of past projects to optimize the default configuration for performance simulations. Energy and Buildings, 73, 83–91.

Hong, T., Chou, S. K., Bong, T. Y. 2000. Building simulation: an overview of developments and information sources. Building and Environment, 35, 347–361.

Morbitzer, C., Strachan, P., Webster, J., Spires, B., Cafferty, D. 2001. INTEGRATION OF BUILDING SIMULATION INTO THE DESIGN PROCESS OF AN ARCHITECTURE PRACTICE. Seventh International IBPSA Conference, Rio de Janeiro, Brazil, August 13-15.

Pino, A., Bustamante, W., Escobar, R., & Pino, F. E. 2012. Thermal and lighting behavior of office buildings in Santiago of Chile. Energy and Buildings, 47, 441–449.

Takizawa H. 1984. Hyojyun-mondai no teian (Office-yo hyojyun-modai). 15th thermal symposium, Architectural Institute of Japan